Dental Materials 40 (2024) 581–592

Contents lists available at ScienceDirect

Dental Materials

journal homepage: www.elsevier.com/locate/dental

Relation between internal adaptation and degree of conversion of short-fiber reinforced resin composites applied in bulk or layered technique in deep MOD cavities

Viktória Néma [a], Sándor Kunsági-Máté [b,c], Zsuzsanna Őri [d,e], Tamás Kiss [f], Péter Szabó [c], József Szalma [g], Márk Fráter [a,1], Edina Lempel [h,*,1]

[a] Department of Operative and Esthetic Dentistry, Faculty of Dentistry, University of Szeged, Tisza Lajos Blvd 64-66, 6720 Szeged, Hungary
[b] Department of Organic and Pharmacological Chemistry, University of Pécs Medical School, Faculty of Pharmacy, Honvéd street 1, 7624 Pécs, Hungary
[c] János Szentágothai Research Center, University of Pécs, Ifjúság Street 12, 7624 Pécs, Hungary
[d] Department of Nutritional Sciences and Dietetics, University of Pécs, Faculty of Health Sciences, Vörösmarty Street 4, 7621 Pécs, Hungary
[e] Department of Physical Chemistry and Materials Science, University of Pécs, Faculty of Sciences, Ifjúság Street 6, 7624 Pécs, Hungary
[f] Department of Pharmacology and Pharmacotherapy, University of Pécs Medical School, Szigeti Street 12, 7624 Pécs, Hungary
[g] Department of Oral and Maxillofacial Surgery, University of Pécs Medical School, Tüzér Street 1, 7623 Pécs, Hungary
[h] Department of Restorative Dentistry and Periodontology, University of Pécs Medical School, Tüzér Street 1, 7623 Pécs, Hungary

ARTICLE INFO

Keywords:
Resin composite
Bulk-fill
Short fiber
Degree of conversion
Internal adaptation
Porosity

ABSTRACT

Objective: The purpose was to evaluate the degree of conversion (DC), internal adaptation (IA) and closed porosity (CP) of short-fiber reinforced resin composites (SFRC) associated with layered or bulk restorative procedures in deep MOD cavities.

Methods: Eighty third molars with standardized MOD cavities (5-mm-depth, 2.5-mm-width) were randomly divided into four groups and restored as follows: 1) bulk SFRC; 2) layered SFRC; 3) flowable bulk-fill resin-based composites (RBC); 4) layered conventional RBC. After one-month wet storage the samples were subjected to micro-computed tomography measurements and scanning electron microscopy to assess the IA and CP. Micro-Raman spectroscopy was used to determine the DC in different depths. Data were subjected to ANOVA and Tukey's post-hoc test, multivariate analysis and partial eta-squared statistics ($p < 0.05$). Pearson correlation coefficient was determined to assess the relationship among the parameters of interest.

Results: Gap/total interface volume ratio ranged between 0.22–0.47%. RBCs applied in bulk revealed significantly lower gap volume ($p < 0.001$) and CP ($p < 0.05$). Each group showed complete detachment on the pulpal and partial on the lateral walls, except for group3. While the highest DC% was achieved by the conventional RBC (87.2%), followed by the flowable bulk-fill (81.2%), SFRC provided the best bottom to top DC ratio (bulk: 96.4%, layered: 98.7%). The effect of factors studied (RBC type, filling technique) on IA and DC was significant ($p < 0.001$).

Significance: Bulk placement of RBCs exhibited lower interfacial gap volume and achieved satisfactory DC without significant correlation between these parameters. Incremental insertion of SFRC had no advantage over bulk placement in terms of IA and DC.

1. Introduction

Dental resin-based composites (RBCs) are the most extensively employed restorative materials in dentistry due to their manifold advantages, including aesthetics and adhesion to dental surfaces. However, a persistent concern associated with these materials is polymerization shrinkage [1]. This shrinkage prompts stress development not only within the restoration itself and at the interface between the restoration and the tooth, but also within the tooth structure [2]. The ramifications of polymerization stress can give rise to a range of

* Correspondence to: Department of Restorative Dentistry and Periodontology, University of Pécs Medical School, Tüzér Street 1, Pécs H-7623, Hungary.
E-mail address: lempel.edina@pte.hu (E. Lempel).
[1] Márk Fráter and Edina Lempel contributed equally to this work

https://doi.org/10.1016/j.dental.2024.02.013
Received 1 October 2023; Received in revised form 8 January 2024; Accepted 12 February 2024
Available online 16 February 2024

clinically relevant issues, such as the formation of marginal and internal gaps, microleakage leading to infiltration by saliva and bacteria, and even cuspal movement [1,3]. These factors, in turn, may compromise the long-term success of the restoration. Among these challenges, the presence of internal voids and gaps proves particularly undesirable due to their detrimental impact on the chemical and mechanical properties of the RBC [4,5]. These voids have the potential to serve as sites for crack initiation, while gaps have the capacity to induce fluid flow within the dentin tubules during activities like mastication or shifts in temperature, thereby resulting in post-operative sensitivity [6]. The magnitude of polymerization stress is subject to the influence of multiple factors, encompassing aspects like cavity dimensions, cavity configuration (expressed through the C-factor, which denotes the ratio between bonded and unbonded surfaces), the constitution of the RBC (including factors such as filler type, size, and filler load), the chosen restorative technique (whether incremental or bulk-fill), and the specifics of the light-curing protocol [7]. The C-factor, in particular, serves as an effective gauge for stress associated with shrinkage, particularly when dealing with scenarios involving comparable cavity volumes. As cavity volume increases, a subsequent escalation in polymerization shrinkage and the resulting gap formation becomes evident [8]. The cavity volume exerts an influence not only on polymerization shrinkage but also on the compromised fracture strength of the tooth, a consequence of the loss of hard tissue [9]. Among different cavity classifications, Class I cavities possess the highest C-factor owing to the absence of marginal ridges and an increased cavity volume. Nevertheless, it is the Class II MOD (mesio-occlusal-distal) cavities that pose the most formidable challenge in the realm of restorative dentistry. To address this challenge, the incremental restorative technique, involving the application of 2 mm thick layers in an oblique or horizontal manner, seeks to mitigate stress arising from polymerization shrinkage. This technique achieves this by systematically modifying the cavity configuration layer by layer, consequently impacting the C-factor [10]. However, the intricacy of this method demands a significant investment of chair time, and the potential for voids to become trapped between layers remains a concern. Hence, the pursuit of a more streamlined approach led to the development of bulk-fill RBCs [11]. These materials possess an extended depth of cure owing to heightened translucency, enabling superior light transmission [12]. Moreover, the composition of bulk-fill materials facilitates alterations in the polymerization process by incorporating highly reactive photoinitiators, stress-relieving monomers, and diverse filler variants, including pre-polymer particles and fiberglass rod segments [11].

A recent advancement aimed at mitigating polymerization shrinkage and its associated stress is the introduction of short-fiber reinforced RBCs (SFRC). SFRC is primarily indicated for dentin replacement in areas bearing high stress due to its distinctive mechanical attributes [13]. This restorative material is composed of a resin matrix, E-glass fibers with randomized orientation, and inorganic particulate fillers. The resin matrix creates a semi-interpenetrating polymer network (semi-IPN), which contributes to improved bonding characteristics and heightened toughness [14]. Literature suggests that SFRC exhibits reduced polymerization shrinkage when compared to conventional RBC [13,14]. Furthermore, SFRC demonstrates a decreased propensity for shrinkage-induced crack formation in MOD cavities, whether applied in bulk or increments [2]. It is worth noting that polymerization shrinkage is managed in alignment with the fibers, preventing contraction along the fiber's length and thereby preserving horizontal dimensions; only the polymer matrix is susceptible to shrinkage. Additionally, the extent of shrinkage and associated stress in RBCs is influenced by their degree of conversion (DC) [13,15].

The degree of conversion (DC) pertains to the extent of monomer transformation into polymers. This parameter exhibits a strong correlation with the mechanical characteristics, biocompatibility, and color stability of RBC restorations, thus being anticipated to influence clinical outcomes [16]. Ensuring satisfactory polymerization in each layer of the RBC is crucial, as inadequate polymerization within the deeper regions of the restoration can contribute to gap formation, marginal leakage, and potential harm to the pulp, which may ultimately result in the failure of the RBC restoration [17,18]. The degree of conversion is influenced by a multitude of factors and constitutes a complex interplay, with notable correlations also existing between DC and shrinkage stress [7,19].

Internal adaptation characterizes the extent to which the RBC restoration conforms to the internal architecture of the tooth. A non-invasive approach involving micro-computed tomography (micro-CT) has been introduced for the investigation of RBCs and their impact on tooth structure. This method enables the quantification of factors such as polymerization shrinkage stress, microleakage, and gap formation [20]. Micro-CT scan data can be utilized to generate a 3D model, facilitating precise volume calculations. Widely acknowledged for its accuracy and reliability, the micro-CT technique serves as to examine the tooth-restoration interface and to quantify voids [1].

The objective of this study was to assess the internal adaptation, porosity, and degree of conversion within short-fiber reinforced bulk-fill RBC restorations, employing either layering or bulk techniques. These findings were then compared to those obtained from high-viscosity conventional layered RBCs and low-viscosity bulk-fill RBCs.

The first hypothesis posited that no discernible differences exist in terms of internal adaptation and porosity between SFRC applications using either the bulk or layered method. Additionally, this hypothesis proposed that SFRC's internal adaptation and porosity are comparable to those of both conventional and bulk-fill RBCs.

The second hypothesis conjectured that no notable distinction exists in the degree of conversion when SFRC is utilized through either the bulk or layering approach. Furthermore, this hypothesis asserted that SFRC's degree of conversion is akin to that of conventional and bulk-fill RBCs.

The third hypothesis hypothesized the absence of correlations among various parameters of interest, including the resultant gap volume, degree of conversion, filling technique, and consistency of the material.

2. Materials and methods

The study protocol was approved by the Hungarian Medical Research Council (approval number: BM/23566–1/2023). The study has been carried out in accordance with the principles of the Declaration of Helsinki. Informed consent was obtained from the subjects. The selected caries-free mandibular third molars – extracted for orthodontic reasons – had the following dimensions: 8–10 mm oro-vestibular diameter, 9–11 mm mesio-distal diameter, and 6–7 mm crown height measured from the cemento-enamel junction. During the entire study period, between the measurements, the teeth were stored in 0.9% saline solution at room temperature.

2.1. Specimen preparation and restorative procedures

MOD cavities were prepared in oro-vestibular width of 2.5 mm and depth of 5 mm. Rounded end parallel diamond bur (881.31.014 FG – Brasseler USA Dental, Savannah, GA, USA) was initially positioned on the occlusal surface halfway between the buccal and lingual cusp tips of the teeth. During the preparation the width was continuously controlled at the cavity base with a digital caliper (Mitutoyo Corp., Kawasaki, Japan) to achieve a uniform 2.5 mm thickness. A periodontal probe (15 UNC Perio Probe, Hu-Friedy Mfg. Co., Chicago, USA) was used to evaluate the 5 mm depth of the cavity at the central portion. Proximal box was prepared in the same dimension (2.5 mm wide and 5 mm deep) as the occlusal cavity providing a continuous and even configuration. Cavosurface margins were prepared in 90° to the tooth surface. The bur was replaced after every tenth teeth.

After preparing the cavities, the teeth were screened for enamel cracks with D-Light Pro (GC Europe, Leuven, Belgium) at 4.3x

magnification in "detection mode". Teeth that showed enamel cracks were replaced with ones that remained free of cracks after cavity preparation. Eigthy crack-free third molars with MOD cavities were then randomly distributed into four groups of 20. All teeth underwent the same restorative procedure according to the followings: prior to 15 s selective etching of enamel with 37% phosphoric acid (GC Ortho Etching Gel (GC Europe, Leuven, Belgium) a Tofflemire matrix (1101 C 0.035, KerrHawe, Bioggio, Switzerland) was securely applied on the tooth. After washing the acid and drying the cavity, a one-step self-etch adhesive (G-Premio Bond, GC Europe) was used based on the manufacturer's instructions and light-cured for 40 s. Both the adhesive and the RBC materials were irradiated with the same quartz-tungsten-halogen light curing unit (Optilux 501, Kerr Corp., Orange, CA, USA). The average irradiance of the light source - monitored before and after the polymerization with a digital radiometer - was 800 ± 40 mW/cm^2.

During the experiments a conventional inhomogen microfilled (G-aenial Posterior), a flowable bulk-fill (SDR) and a high-viscosity short-fiber-reinforced RBC (EverX Posterior) were used. Table 1 shows the materials, their manufactures, and compositions used in the study.

In Group 1 (n = 20) the cavities were restored with one bulk SFRC layer in 4 mm thickness, leaving 1 mm for occlusal covering with conventional RBC. The SFRC was light-cured for 40 s, the superficial layer for 20 s

In Group 2 (n = 20) the cavities were restored with approximately 2 mm thick oblique layers of SFRC by successive cusp build-up, overall in 4 mm depth. The RBC layers were light-cured for 40. The top surface was covered with 1 mm thick conventional RBC and was light-cured for 20 s

In Group 3 (n = 20) the cavities were restored with approximately 2 mm thick oblique layers of conventional RBC by successive cusp build-up. The layers were light-cured for 40 s except the surface layer, which was polymerized for 20 s

In Group 4 (n = 20) the cavities were restored with a 4 mm thick flowable bulk-fill RBC layer, light-cured for 40 s, meanwhile the uppermost 1 mm was covered with conventional RBC and was light-cured for 20 s

Fig. 1 shows the schematic drawing of the experimental groups.

All restorations were finished with a fine diamond bur (FG 7406–018, Jet Diamonds, Ft. Worth, TX, USA and FG 249-F012, Horico, Berlin, Germany) and polished with an aluminum oxide polisher (One-Gloss PS Midi, Shofu Dental GmbH, Ratingen, Germany). The restored teeth were stored in physiological saline solution (Isotonic Saline Solution 0.9% B.Braun, Melsungen, Germany) in an incubator (mco-18aic, Sanyo, Japan) at 37 °C until the start of the experimental procedures (one month).

2.2. Micro-computed tomography measurements – 3D internal adaptation and porosity

To analyze the 3D internal adaptation (IA) and closed pore (CP) volume micro-computed tomography (micro-CT) scans were performed (Skyscan 1176 Control Program: version 1.1 (build 12), Bruker, Kontich, Belgium) of the 80 samples after one month from the polymerization. Each specimen was positioned in a sample holder and scanned for 50 min. After scanning, the samples were stored in dark in an incubator (Cultura, Ivoclar Vivadent, Schaan, Liechtenstein) in 37 °C physiological saline solution. The parameters, such as operating energy (80 kV, 310 μA), resolution (8.74 μm/slice), rotation step (0.7°), exposure time (1500 ms), and the filter (Al 1 mm) for the micro-CT device were kept constant for all measurements. Raw image reconstruction and prepare for analysis was performed with SkyScan reconstruction program (NRecon, v.1.7.4.2, Bruker, Kontich, Belgium). The raw images were uniformly reconstructed and multiplanar image sequences were created. Images were converted to 1404 × 1404 pixel resolution in * .bmp format. To evaluate the interfacial gap between the cavity walls and restoration the reconstructed image sequences were rotated to a standardized position so that the plane of the image slices was perpendicular to the vertical axis of the restoration (DataViewer: version 1.5.6.2 64-bit). After the raw image acquisition and reconstruction, the following workflow was applied (Fig. 2 B) of each tooth to analyze the 3D microarchitecture of the images (CT Analyser: version 1.20.8.0 +, Bruker, Kontich, Belgium): identification and designation of region of interest (ROI) at the tooth-restoration interface (including 0.1 mm tooth and 0.1 mm restoration along the interface); binary selection to allow easy separation of the object from the background; image filtering for noise reduction to allow easy recognition of gap at the interface by the software; thresholding, by selecting areas with the same density as air; 3D analysis along the interface of the entire restoration (CTvox: version 3.1.1 r1191, 64-bit) (Fig. 2). The ratio of gap and ROI was calculated and given in percentage.

To assess the CP volume, the entire RBC specimen was included to the region of interest (ROI). The pores were calculated using the gray-scale images processed with a Gaussian low-pass filter for noise reduction. A global threshold was used to process the gray level ranges to provide an imposed image of exclusively black and white pixels. The CP volume relative to the total volume of the RBC samples was calculated (%) by measuring the internal voids and specimen volumes of each RBC sample.

2.3. Scanning electron microscopy – Internal marginal adaptation

After one month storage in physiological saline solution the roots of five restored teeth from each group were removed 2 mm below the cemento-enamel junction and the crowns were cross-sectioned through their centers in a mesio-distal direction, using a water-cooled diamond blade (Isomet Diamond Wafering Blade, no. 11–4244, Buehler Ltd., Lake Buff, IL, USA) (Fig. 3).

The halves were polished using a sequence of aluminum-oxide abrasive discs from coarse (50–90 μm) to superfine (1–7 μm) (Sof-Lex

Table 1
Study groups, materials, application methods, manufacturers, and composition of the investigated resin based composites.

Group	Application method	Material	Manufacturer	Shade	Organic matrix	Filler	Filler loading (vol%/wt%)
Group 1 G-aenial_Layered	HV conventional RBC in 2×2mm incremental layers	G-aenial Posterior	GC Europe, Leuven, Belgium	A3	UDMA, TCDDD, DMA	F-Al-silicate, Sr-glass, lanthanide-F	65.0/77.0
Group 2 * EverX_Bulk	HV SFRC 4 mm bulk layer	EverX Posterior	GC Europe, Leuven, Belgium	U	BisGMA, TEGDMA, PMMA	0.7 μm barium glass (65.2%), 17μmx1-2 mm short E-glass fibers (9%)	53.6/74.2
Group 3 * EverX_Layered	HV SFRC in 2×2mm incremental layers						
Group 4 * SDR_Bulk	LV bulk-fill RBC in 4 mm	Surefil SDR Flow+	Dentsply, Milford, DE, USA	U	Modified UDMA, TEGDMA, DMA, TMA	4.2 μm Ba-Al-F-B silicate glass, Sr-Al-F silica, YbF	47.4/70.5

Abbreviations: RBC: resin based composite; SFRC: short-fiber reinforced resin composite; HV: high viscosity; LV: low viscosity; U: universal; vol%: volume%; wt%: weight%; BisGMA: bisphenol-A diglycidil ether dimethacrylate; TEGDMA: triethylene glycol dimethacrylate; PMMA: polymethyl methacrylate; UDMA: urethane dimethacrylate; DMA: dimethacrylates, TMA: trimethacrylates; TCDDD: Tricyclodecane dimethanol dimethacrylate; * 1 mm covering with G-aenial Posterior RBC

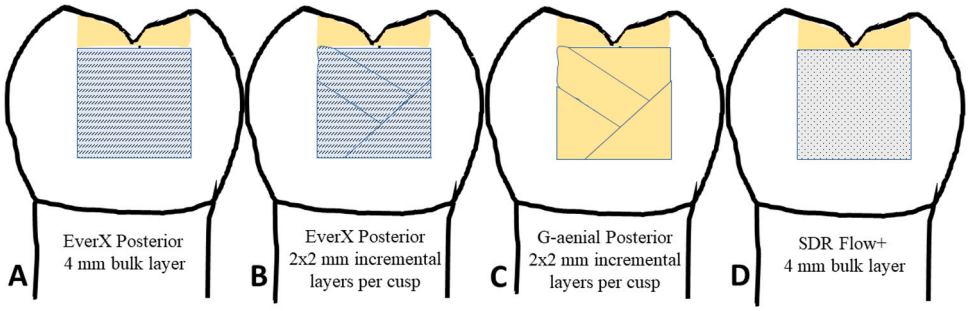

Fig. 1. Schematic figure representing the test groups. (A) Group 1 (EverX_Bulk): bulk-fill short-fiber reinforced resin composite (EverX Posterior) covered with conventional resin composite (G-aenial Posterior); (B) Group 2 (EverX_Layered): obliquely layered short-fiber reinforced resin composite (EverX Posterior) covered with conventional resin composite (G-aenial Posterior) (C) Group 3 (G-aenial_Layered): obliquely layered conventional resin composite (G-aenial Posterior); (D) Group 4 (SDR_Bulk): bulk-fill SDR which is covered with conventional resin composite (G-aenial Posterior).

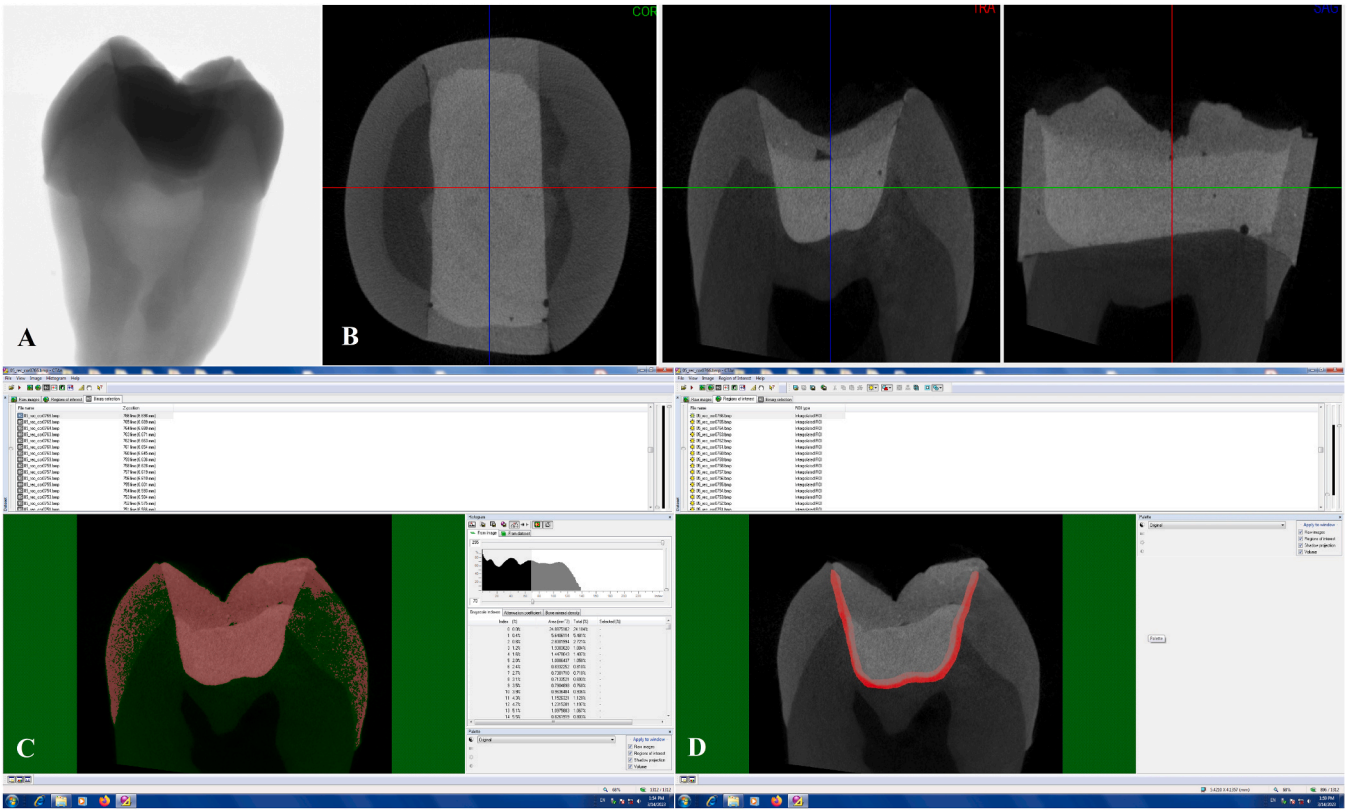

Fig. 2. Workflow of 3D internal marginal adaptation analysis: raw image (A), multiplanar image sequences (B), reconstructed image (C), identification and designation of region of interest (ROI) on the axial slices (D).

Polishing Discs, 3 M, St. Paul, MN, USA) and felt discs (Enamel Plus Shiny FD Interproximal Felt Discs, Micerium, Avegno, Italy) with diamond containing pastes (3 μm - Shiny A and 1 μm - Shiny B, Micerium, Avegno, Italy). The finishing and polishing procedure was performed under constant irrigation with cooled (7 °C) physiologic saline. Specimens were cleaned in ultrasonic bath for 10 min to remove debris (Emmi-20HC, eMAG, Salach, Germany). The scanning electron microscopy (SEM) examination of the dentin-restoration interface on the pulpal wall became possible on this vertical section. One halve of the teeth were further cross-sectioned horizontally (Fig. 3) and polished with the above described method. Horizontal sectioning provided access to examine the dentin-restoration interface on the lateral wall. (The other vertical halve was used for Raman measurements.) In order to reduce shrinkage and gap formation due to drying for SEM evaluation, the teeth were immersed in hexamethyldisilazane (HMDS, Millipore Sigma, Burlington, MA, USA) for 10 min, then were left on filter paper in a covered glass vial, and air-dried at room temperature. Thereupon the specimens were sputter-coated with gold to a thickness of 50 nm in a vacuum evaporator (Auto-fine coater, JFC-1300, JEOL, Tokio, Japan) in order to analyze the presence of internal interfacial gaps under scanning electron microscope (SEM) (JEOL JSM-IT500HR, JEOL, Tokio, Japan).

Micrographs were taken from the vertical and horizontal cutting surfaces at standardized magnifications (200X, 400X, 800X), in order to document the bonded internal interface. 2000 μm section of the lateral and the pulpal wall were marked out along the dentin-restoration interface (Fig. 3) to observe and measure the length of the interfacial gaps. The ruler tool of the build in SEM operation control software was used to determine the length of debonded segments along the designated dentin-restoration interface. The SEM image scale bar was used for calibration and the lengths of debonded segments were obtained in

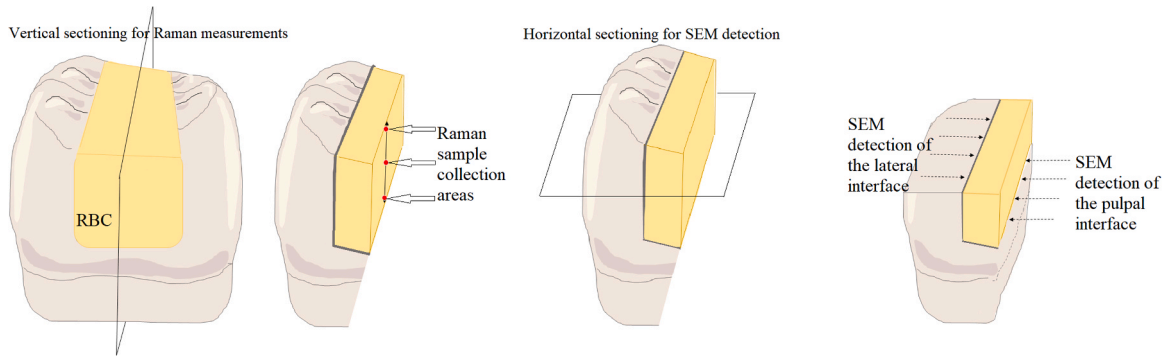

Fig. 3. Schematic figure of sample preparation for micro-Raman and scanning electron microscopy (SEM) measurements. The resin-based composite (RBC) fills the cavity which has exactly the same width (2.5 mm) and depth (5 mm) occluso-proximally. Mesio-distal vertical sectioning provided the sample for micro-Raman measurements at three different points along the occluso-pulpal dimension of the RBC. Horizontal sectioning of the halves provided the sample for SEM measurements along the dentin-restoration interface at a 2000 μm section of the lateral and the pulpal wall.

micrometers. Data were summed and the total unbonded interface length as a function of the total length of designated section was calculated [(unbonded length/total length) x100 = interfacial gap percentage = IG%].

2.4. Micro-Raman spectroscopy measurements – degree of conversion

The vertically cross-sectioned teeth (n = 5 per group) (Fig. 3) were mounted on a universal holder that enabled translation along the sample, providing exposure at different depths to the excitation laser light. One-month post-cure DC values were evaluated with a confocal Raman spectrometer (Labram HR 800, HORIBA Jobin Yvon S.A.S., Longjumeau Cedex, France). Raman spectra were collected from three depths of the restoration: 0.5 mm below the surface (top); at the geometric center of the distance between the top and bottom of the sample (middle); and 0.5 mm occlusally from the bottom of the cavity (bottom). During the measurements, the exposed sample surface was about 0.2 mm in diameter with an integration time of 10 s

The average of ten measurements were collected from three points per each region (top, middle, and bottom). The parameters of the measurements were set according to the following: 20 mW He-Ne laser excitation with 632.817 nm wavelength, magnification x 100 (Olympus UK Ltd., London, UK), spatial resolution ~15 μm, spectral resolution of ~2.5 cm^{-1}. Both diffraction gratings of 600 l/mm and 1800 l/mm are applied. Peltier-cooled CCD (1024 ×256 px) detector is used. Spectra were also taken from the uncured RBCs as reference. Raman data were analyzed between 1440 and 1660 cm^{-1}. The spectra were processed (baseline correction, background correction, and wavelength range selection) using LabSpec 5.0 (HORIBA Jobin Yvon S.A.S., Longjumeau Cedex, France) dedicated software for the analysis and post-processing of the spectra. Eight ordered polynomial fit followed by subtraction from the raw data are applied. The Raman vibrational stretching modes at 1458, 1609, and 1640 cm^{-1} were fitted with Lorentzian shapes in order to obtain the absorption peak heights using Origin software package (Origin, Microcal Software Inc., Northampton, MA, USA). DC calculation was performed by comparing the relative change of the band at 1640 cm^{-1}, representing the aliphatic C=C bonds to a reference band, before and after the polymerization. For EverX Posterior the aromatic C=C band at 1609 cm^{-1} was used as a reference. Due to the lack of the aromatic C=C bonds in the case of G-aenial and SDR, reference band at 1458 cm^{-1} (CH_2 deformation) were used [21].

DC values were calculated by including the integrated intensities of aliphatic C=C and reference bands in the following formula:

$$DC\% = (1 - (R_{cured}/R_{uncured}))x100$$

where R is the ratio of peak intensities at 1640 cm^{-1} and 1609 cm^{-1} or 1458 cm^{-1} (as references) associated to the unconjugated and conjugated carbon bonds or CH_2 deformation in non-polymerized and polymerized RBCs, respectively.

2.5. Statistical analysis

Previous study results [22,23] and sample size formula [24] were used to estimate sample size for micro-CT (IA) and micro-Raman spectroscopy (DC) measurements.

$$\text{Sample size formula}: n = \frac{(z_{1-\frac{\alpha}{2}} + z_{1-\beta})^2 (s_1 + s_2)^2}{(M_1 - M_2)^2}$$

[z = standard score; α = probability of Type I error at 95% confidence level = 0.05; $z_{1-\alpha/2}$ = 1.96 for 95% confidence; β = probability of Type II error = 0.20; 1 − β = the power of the test = 0.80; $z_{1-\beta}$ = value of standard normal variate corresponding to 0.80 value of power = 0.84; s_1 = standard deviation of the outcome variable of group 1 = 1.5; s_2 = standard deviation of the outcome variable of group 2 = 0.8; M_1 = mean of the outcome variable of group 1 = 67.4; M_2 = mean of the outcome variable of group 2 = 64.5. For IA determination the s_1 = 0.12; s_2 = 0.18; M_1 = 0.71; M_2 = 0.42. For DC determination the s_1 = 1.5; s_2 = 0.8; M_1 = 67.4; M_2 = 64.5. The predicted sample size (n) for IA and DC measurements was found to be a total of 8.4 and 4.9 samples per group, respectively. According to the calculation n = 20 and n = 5 per group sample size was selected for IA/CP and DC measurements, respectively.

The statistical analyses were performed with SPSS (Version 28.0; IBM, Armonk, NY, USA). Kolmogorov-Smirnov test was applied to test the normal distribution of the data, followed by a parametric statistical test. The DC values, internal gap volume, and closed porosity volume of the samples were compared with one-way analysis of variance (ANOVA). Tukey's post hoc adjustment was used for multiple comparison. Univariate analysis of variance was applied to test the effect of the *material* (RBC type), *filling method* (bulk vs. layered) and their interaction on the IA, furthermore the *material, depth (top, middle, bottom* of the sample), and their interaction on the DC. A Pearson product-moment correlation was run to determine the strength of association between the parameters of interest, such as IA, DC, filling technique (bulk vs. layered), and consistency. P values below 0.05 were considered statistically significant.

3. Results

3.1. Micro-computed tomography measurement - 3D internal adaptation and porosity

The ratio of interfacial gap volume to the total interface volume (ROI for IA) is presented in Fig. 4. The largest gap formation in relation to the

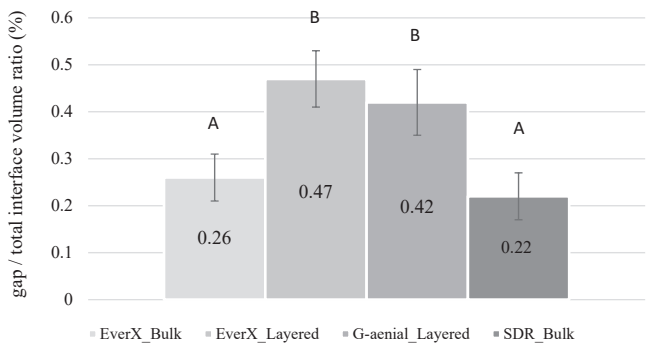

Fig. 4. Ratio of interfacial gap volume to the total volume of the designated examined interfacial area (region of interest, ROI) evaluated with 3D micro-computed tomography measurements. Different capital letters indicate a statistically significant difference according to the one-way ANOVA and Tukey's post hoc tests.

examined total interface was detected in the SFRC group filled with layered technique, meanwhile SDR_Bulk revealed the best IA. However, there was no statistically significant difference between the layered [EverX_Layered vs. G-aenial_Layered: $p = 0.124$, 95% Confidence Interval (CI): − 0.01–0.11] and the bulk-filled groups (EverX_Bulk vs. SDR_Bulk: $p = 0.42$, 95% CI: −0.02–0.09). Regarding the comparison between the bulk-filled vs. layered groups, EverX_Bulk and SDR_Bulk showed statistically significantly lower gap formation compared to EverX_Layered and G-aenial_Layered (EverX_ Layered vs. EverX_Bulk: $p < 0.001$, 95% CI: 0.15–0.27; G-aenial_Layered vs. EverX_Bulk: $p < 0.001$, 95% CI: 0.11–0.22; EverX_Layered vs. SDR_Bulk: $p < 0.001$, 95% CI: 0.19–0.30; G-aenial_Layered vs. SDR_Bulk: $p < 0.001$, 95% CI: 0.14–0.25).

According to the 3D evaluation, the volume of IP relative to the total volume of the RBC sample showed significantly higher values for the layered samples (G-aenial_Layered: 0.15%; EverX_Layered: 0.17%) compared to the bulk RBCs (EverX_Bulk: 0.11%; SDR_Bulk: 0.12%). The one-way ANOVA and the Tukey's post-hoc test revealed significant difference between G-aenial_Layered vs. EverX_Bulk ($p = 0.011$; 95% CI: 0.01–0.07), and G-aenial_Layered vs. SDR_Bulk ($p = 0.045$; 95% CI: 0.01–0.07), furthermore, EverX_Layered vs. EverX_Bulk ($p < 0.001$, 95% CI: 0.02–0.09) and EverX_Layered vs. SDR_Bulk ($p = 0.002$, 95% CI: 0.01–0.08). No significant differences could be detected between the samples made with the layering technique ($p = 0.659$, 95% CI: −0.05–0.02) or between the bulk groups ($p = 0.938$, 95% CI: −0.04–0.03). Univariate analysis of variance showed a significant effect of the *material* (RBC type) and *filling method* regarding the IA [$F(3,76) = 61.6$, $p < 0.001$; $F(1,78) = 166.1$, $p < 0.001$, respectively]. The partial eta-squared was considered to be moderately large ($\eta p^2 = 0.71$ and 0.68, respectively). However, their interaction (*material x filling method*) had an insignificant effect on the gap formation [$F(1,76) = 2.6$, $p = 0.108$; $\eta p^2 = 0.03$].

3.2. Scanning electron microscopy – internal adaptation

Complementary SEM analysis of the pulpal and lateral interfaces of the dentin-RBC revealed comparable performance of the investigated RBC types and application methods on the pulpal floor (Fig. 5A), however, distinct results were visualized on the lateral walls (Fig. 5B).

Fig. 6 demonstrates the IG% at the pulpal floor and lateral wall of the examined groups. Interfacial defects at the pulpal interface were detected in similar length (IG% = 100%) for each investigated groups. The interfacial defects mostly developed between the adhesive-RBC interface. Well sealing (IG% = 0%) internal adaptation was demonstrated at the lateral interfaces of SDR_bulk. SEM images of EverX_layered demonstrated 70% of IG, meanwhile G-aenial_layered and EverX_bulk groups showed 40% of gap formation along the examined lateral interfacial section. The gaps visible along the lateral walls were formed between the adhesive layer and the dentin.

3.3. Micro-Raman spectroscopy measurements – degree of conversion

Regarding the DC at the top, middle, and bottom surfaces of the

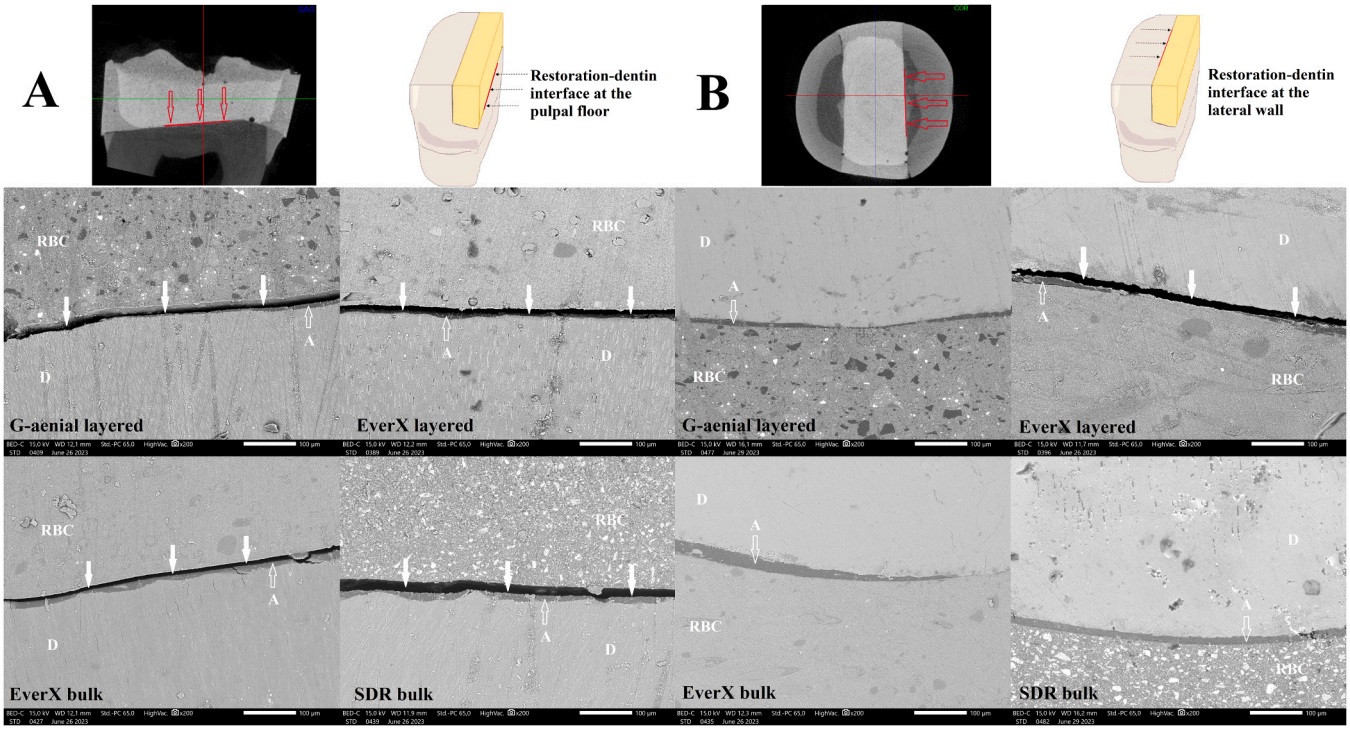

Fig. 5. Representative scanning electron microscopy images (200X magnification) of restoration-dentin interfaces at the pulpal floor (A) and lateral wall (B) of the investigated resin-based composites (RBC) applied with layered or bulk technique. Bold white arrows show the interfacial gap; D – dentin, A – adhesive layer.

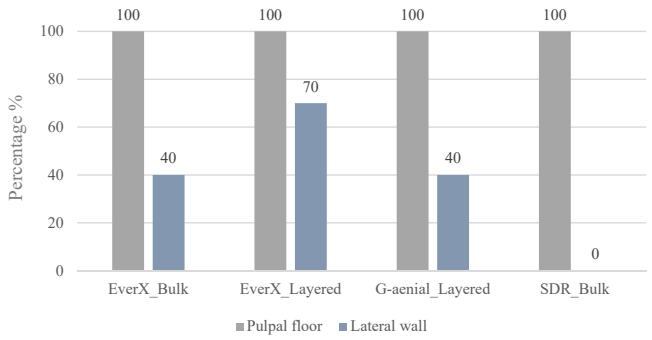

Fig. 6. Interfacial gap % (gap/total measured surface) at the pulpal floor and lateral wall of the investigated cavities restored with short-fiber reinforced, conventional and flowable bulk-fill resin composites applied in bulk or incremental technique evaluated with scanning electron microscope.

samples, percentages ranged between 77.1–90.7%, 75.9–87.8%, and 74.3–83.2%, respectively. The highest DC values were achieved by G-aenial_Layered group, while EverX_Bulk provided the lowest DC values. When comparing the DC values measured at the top, middle, and bottom of the samples, it was found that both EverX_Bulk and EverX_Layered reached almost the same degree of polymerization throughout the entire depth (Fig. 7). The bottom to top DC ratio (R-DC) of EverX_Bulk and EverX_Layered was 96.4% and 98.7%, respectively. The R-DC of G-aenial_Layered (91.7%) was almost the same as that of SDR_Bulk (91.5%). DC values at the top and bottom showed statistically significant difference in the groups of G-aenial_Layered (95% CI: 1.5–13.4) and SDR_Bulk (95% CI: 2.3–11.7). Furthermore, significant difference was also found between the DC% at the middle and bottom region (95% CI: 0.9–10.3) of SDR_Bulk (Fig. 7).

The comparison of the DC values of the investigated groups by region is presented in Table 2. Statistically significant differences were found among DC% of all groups at the top and middle parts of the samples ($p < 0.05$), except EverX_Bulk and EverX_Layered ($p = 0.961$). At the bottom of the samples, more groups showed similar DC values ($p > 0.05$), except SDR_Bulk vs. G-aenial_Layered ($p = 0.008$), EverX_Bulk vs. G-aenial_Layered ($p < 0.001$), and EverX_Layered vs. G-aenial_Layered ($p = 0.008$).

Mixed model ANOVA revealed, that the effect size of *material* (RBC type) was the highest on the top DC values [$F(3,32) = 25.07$, $p < 0.001$] followed by the DC% at the middle region [$F(3,32) = 18.47$, $p < 0.001$] and then by the DC% at the bottom [$F(3,32) = 8.83$, $p < 0.001$]. The partial eta-squared was considered to be moderately large for each

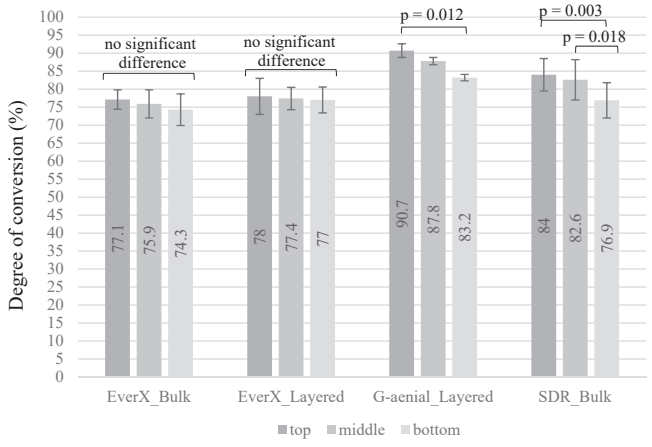

Fig. 7. Differences in degree of conversion at the top, middle, and bottom region of the samples within the investigated groups. (Comparison was performed using one-way ANOVA and Tukey's post hoc tests).

region ($\eta p^2 = 0.70$, 0.63, and 0.45, respectively). The analysis of effect size of the *depth* (top, middle, and bottom region) on the DC values resulted in different findings in the examined groups. The effect size of the depth had a significant impact on DC% of SDR_Bulk [$F(2,24) = 7.66$, $p = 0.003$] and Gaenial_Layered [$F(2,24) = 5.04$, $p = 0.015$] with a moderately large partial eta-squared ($\eta p^2 = 0.39$ and 0.30, respectively). The effect of depth on DC% in EverX_Bulk and EverX_Layered seemed to be irrelevant [$F(2,24) = 1.27$, $p = 0.298$, $\eta p^2 = 0.09$ and $F(2,24) = 1.13$, $p = 0.339$, $\eta p^2 = 0.09$, respectively].

Considering all the investigated groups, the Pearson correlation coefficient revealed, that the strength of association between IA and DC is small and insignificant [$r(78) = 0.14$, $p = 0.228$], while, the filling technique (bulk vs. layered) has a strong association with IA [$r(78) = 0.83$, $p < 0.001$] and small association with DC [$r(78) = 0.34$, $p = 0.002$]. Since the two bulk groups (EverX_Bulk and SDR_Bulk) had different consistency (EverX was condensable, SDR was flowable), Pearson correlation was run to detect the relation between IA and consistency, furthermore DC and consistency. The results showed strong association between IA and consistency [$r(38) = 0.86$, $p < 0.001$], while medium between DC and consistency [$r(38) = 0.39$, $p = 0.013$]. Both in IA and DC the flowable consistency contributed to a more favorable outcome.

4. Discussion

Despite continuous advancements in the properties of RBCs and adhesives over the past decade [25], achieving optimal integrity and sealing capability for RBCs remains a notable challenge. Inadequate adaptation can give rise to issues like microleakage, secondary caries, discoloration, fracture, and ultimately, restoration loss [26]. The effectiveness of tooth-RBC adhesion is influenced by a multitude of factors, including DC, elastic modulus, volumetric polymerization contraction, resulting shrinkage stress, C-factor, curing protocol, and the complex interplay between RBCs, adhesives, and tooth tissues [7,27]. The primary objective of this study was to scrutinize the internal adaptation, porosity, and degree of conversion within SFRC, employed either in bulk or incremental applications. These findings were then juxtaposed with those from a high-viscosity conventional layered RBC and a low-viscosity bulk-fill RBC. To ensure the exclusion of various influencing factors, uniformity was maintained across specimen parameters, encompassing cavity type and size, curing methodology, and adhesive system. The sole variable altered within the experiment pertained to the type of RBC and/or the method of application.

In this *ex vivo* study, three hypotheses were tested. The first hypothesis assumed that SFRC does not differ in terms of internal adaptation and porosity using the bulk or layering technique, as well as conventional or bulk-fill RBCs. The first hypothesis was partially rejected, as the results of the present study showed that although debonding of the RBCs occurred in all the tested samples, its pattern varied according to the RBC type and application method.

The second hypothesis, which anticipated no difference in the DC if SFRC is used in bulk or layering method, or when compared to conventional or bulk-fill RBCs, was partially rejected. A statistically significant difference was detected in DC among the investigated groups, except for EverX_Bulk vs. EverX_Layered, which showed statistically similar DC values in each investigated region of the restoration (top, middle, and bottom).

The third hypothesis, which assumed that there is no correlation among the parameters of interest, was partially rejected. Strong correlations were detected between IA/filling technique and IA/consistency, as well as a moderate correlation between DC/consistency. Additionally, a small correlation was noted between DC/filling technique. However, the hypothesis regarding the DC/IA relationship should be accepted due to the insignificant association found by the Pearson correlation test.

Utilizing micro-CT technology, we were able to precisely measure the volume of the internal gap and porosity [28]. Our findings align with

Table 2
Comparison of the degree of conversion (DC%) between the experimental groups on the top, middle, and bottom of the samples (One-way ANOVA and Tukey's post hoc tests; * statistically significant).

Region of measurement	Compared groups			Mean DC% difference	95% CI		p-value
					Lower	Upper	
Top	SDR_Bulk	vs.	EverX_Bulk	6.9	2.1	11.7	0003 *
	SDR_Bulk	vs.	EverX_Layered	6.0	1.2	10.8	0,01 *
	SDR_Bulk	vs.	G-aenial_Layered	-6.7	-11.5	-1.9	0004 *
	EverX_Bulk	vs.	EverX_Layered	-0.9	-5.7	3.9	0.961
	EverX_Bulk	vs.	G-aenial_Layered	-13.6	-18.4	-8.8	< 0001 *
	EverX_Layered	vs.	G-aenial_Layered	-12.7	-17.5	-7.9	< 0001 *
Middle	SDR_Bulk	vs.	EverX_Bulk	6.7	1.9	11.5	0004 *
	SDR_Bulk	vs.	EverX_Layered	5.2	0.4	10.0	0031 *
	SDR_Bulk	vs.	G-aenial_Layered	-5.2	-10.0	-0.4	0031 *
	EverX_Bulk	vs.	EverX_Layered	-1.5	-6.3	3.3	0.828
	EverX_Bulk	vs.	G-aenial_Layered	-11.9	-16.7	-7.1	< 0001 *
	EverX_Layered	vs.	G-aenial_Layered	-10.4	-15.2	-5.6	< 0001 *
Bottom	SDR_Bulk	vs.	EverX_Bulk	2.7	-2.2	7.6	0.446
	SDR_Bulk	vs.	EverX_Layered	0.0	-4.9	4.8	1.000
	SDR_Bulk	vs.	G-aenial_Layered	-6.2	-11.1	-1.3	0008 *
	EverX_Bulk	vs.	EverX_Layered	-2.7	-7.6	2.1	0.435
	EverX_Bulk	vs.	G-aenial_Layered	-8.9	-13.8	-4.1	< 0001 *
	EverX_Layered	vs.	G-aenial_Layered	-6.2	-11.1	-1.3	0008 *

previous research, which similarly concluded that none of the tested materials succeeded in preventing gap formation [29]. While gaps were evident across all samples, variations existed in their volume. A more pronounced degree of internal gap (IG) was discernible in groups restored through incremental techniques (EverX_Layered and G-aenial_Layered) when juxtaposed with bulk-filled groups (EverX_Bulk and SDR_Bulk), where a 4-mm increment was employed. Notably, the application of SFRC using both bulk and layered methods revealed greater gap formation, with the layered application exhibiting particularly heightened gap formation. Through Pearson correlation analysis, a robust and significant association between filling technique and internal adaptation was evident. Conversely, Furness et al. reported a contrasting observation, noting that bulk-fill products exhibited slightly improved outcomes when utilized in an incremental mode compared to being placed within a 4-mm increment [29].

To validate the findings derived from the micro-CT measurements, all specimens underwent sectioning and subsequent evaluation through SEM. Concerning the SEM visualization of internal adaptation, a noteworthy correlation emerged between gap volume and the percentage of internal gap (IG%). In congruence with these results, a consistent pattern emerged across all examined groups, revealing gap development at the pulpal floor, specifically between the RBC and the adhesive layer. Our observations align with existing research, which highlights the pulpal floor as the region most susceptible to gap formation [29]. This propensity is attributed to the orientation of shrinkage vectors, directed towards the free or unbonded surface, consequently leading to detachment along the pulpal wall [30]. Building upon these findings, Han and Park's study also established that in class II RBC restorations, the internal adaptability of the gingival floor within the proximal box and the pulpal floor of the cavity exhibited poorer outcomes compared to the buccal and lingual walls [20]. This outcome was explained by the discrepancy between the occluso-gingival height and the bucco-lingual width. As the RBC undergoes polymerization, the shrinkage vector could be more pronounced along the occluso-gingival axis compared to the bucco-lingual axis [20]. Diverging perspectives emerge when considering the characteristics of dentinal tubules within a deep cavity floor in contrast to those present in the outer superficial dentin. Notably, the diameters of dentinal tubules vary, consequently impacting the volume of fluid-filled tubule lumens near the pulpo-dentinal junction. Moreover, the peritubular dentin either assumes a thinner composition or is absent altogether [31]. SEM images consistently revealed that in all examined groups, separation at the pulpal floor occurred between the adhesive layer and the RBC. This phenomenon finds explanation in the osmosis effect, as elucidated by Van Landuyt et al. [32]. According to this theory, the oxygen inhibition layer present at the uppermost region of the adhesive forms a hypertonic zone due to the presence of uncured monomers. In contrast, the dentin, characterized by water-filled tubules and collagen-bound water, represents a hypotonic region. Consequently, water diffusion (osmosis) transpires through the cured adhesive, leading to the emergence of water droplets on the adhesive surface [32]. The functional monomers inherent to single-step self-etch adhesives assume the role of semi-permeable membranes due to their robust hydrophilic nature. This attribute contributes to the occurrence of phase separation at the adhesive-RBC interface [33]. Under these circumstances, conditions for dentin bonding are suboptimal, rendering the pulpal floor potentially less conducive to dentin bonding when compared to the occlusal sections of the buccal and lingual walls. Variations in the orientation of dentinal tubules further contribute to these distinctive bonding characteristics across different regions.

In agreement with the aforementioned phenomenon, our findings substantiated reduced gap occurrences on the lateral walls, though notable differences emerged among the groups. Within the EverX_Layered group, 70% of the lateral interfaces exhibited gap formation, while the IG% for EverX_Bulk and G-aenial_Layered was 40%, and no gaps were identified on the lateral walls of SDR_Bulk specimens. Although micro-CT volumetric measurements revealed no significant distinctions between the layered and bulk placements, it is plausible that the dissimilarities in IG% as detected by SEM, and the gap volume quantified through micro-CT, stem from variations in the size of interfacial gaps formed. However, contrary to our observations, prior investigations have suggested that the incremental technique yields superior internal adaptation compared to the bulk-fill approach [11,26], or results in an equivalent proportion of gap-free internal interfaces [29, 34]. Across numerous experiments, a robust and positive correlation has been established between internal interfacial gap formation and polymerization shrinkage stress [1,11,20]. Evaluation of shrinkage vectors has revealed larger mean values in cases of bulk application compared to incremental filling [35]. The magnitude of polymerization shrinkage stress is subject to the influence of multiple factors, encompassing filler content, resin system, shrinkage volume, elastic modulus, resin flow, adhesion to the tooth, compliance of cavity walls, and cavity configuration factor [20,36].

Our disparate outcomes may, in part, be attributed to the fact that our measurements were conducted after a one-month period of water storage subsequent to polymerization. Post-polymerization, further conversion and subsequent shrinkage/stress could transpire [37].

Furthermore, water absorption, coupled with resultant swelling and potential hydrolytic degradation, could introduce distinct findings in contrast to immediate post-polymerization assessments [2,38]. Artificial aging has been demonstrated to lead to escalated marginal gap formation and a reduction in the internal adaptation of RBCs [39]. However, the absorption of water by RBCs during storage might act as a compensatory mechanism for the effects of initial polymerization shrinkage and shrinkage stress [40]. In concurrence with our findings, Park et al. showcased a higher degree of gap expansion for layered RBCs following artificial aging compared to bulk-fill counterparts [39]. The infiltration of water into a polymeric structure is subject to the influence of multiple factors, including the degree of conversion (DC) [41], cross-link density [42], and the hydrophilic nature of the network [43]. Sorption values have exhibited a noteworthy negative correlation with the extent of filler loading [44]. In this study, among the investigated RBCs, G-aenial exhibited the highest filler load, followed by EverX, and subsequently, SDR. This hierarchy of filler content concurs with the observed trends in internal adaptation (IA). Water sorption, primarily associated with the polymeric phase, is influenced by filler content; as filler content increases, this phenomenon diminishes due to the inverse correlation between filler content and the polymeric matrix [44]. An additional explanation may be attributed to the matrix component of RBCs. Elevated levels of triethylene glycol dimethacrylate (TEGDMA) and bisphenol-A glycidyl dimethacrylate (BisGMA) - fundamental constituents of EverX Posterior and SDR - can lead to heightened water absorption, resulting in swelling and plasticization of the RBC [45]. However, this rationale fails to elucidate the disparities observed between the bulk and incrementally applied SFRC samples. Kaisarly et al. suggested that clinicians opt for incremental application of bulk-fill RBCs to mitigate stress on the bond, thereby preserving interfacial integrity [35]. Our findings concerning SFRC do not support this claim, as EverX Posterior, when applied using the incremental technique, exhibited inferior internal adaptation compared to the bulk technique. A distinguishing feature of EverX lies in its specialized filler load, specifically the inclusion of short E-glass fibers. These fiber-reinforced RBCs have demonstrated greater hygroscopic expansion when contrasted with other fiber-reinforced or particulate-filled RBCs [46]. Viewed from a different perspective, the haphazardly oriented glass fibers may possess the capacity to mitigate shrinkage/stress. As polymerization shrinkage along the glass fibers is thought to be constrained, occurring exclusively perpendicular to the fibers, a more advantageous fracture resistance of the restored teeth may result [9,13]. When SFRC is introduced into the cavity via a capsule in a 4 mm bulk quantity, both the resin matrix molecules and the randomly oriented fibers are somewhat aligned in the direction of flow [47]. Yet, when employing the incremental technique with SFRC, the layers must be compacted against the cavity walls, potentially inducing a coerced parallel orientation of the fibers. This shift in fiber alignment may alter the trajectory of shrinkage vectors, potentially yielding increased shrinkage perpendicular to the fibers [15]. This could contribute to a reduced presence of gap-free interfaces and/or a higher gap volume. An assessment of shrinkage vectors divulged that subsequent increments become well-bonded to the oxygen-inhibited layer of preceding increments, which are drawn upward during layering [48]. Additionally, the lower DC of the first increment would apparently maintain greater flexibility in moving upwards [48]. Conversely, the heightened translucency of 2 mm SFRC facilitates deeper light penetration during curing, culminating in amplified shrinkage vector values and, consequently, an elevated upward displacement of the first increment [49].

The smallest gap volume, as discerned from the present micro-CT assessment, was observed in the context of the flowable SDR. This particular RBC stands out due to its heightened flexibility and diminished shrinkage stress, attributes attained through the incorporation of patented modified urethane dimethacrylate and the utilization of a polymerization modulator [35]. Several studies have corroborated that this low-viscosity bulk-fill exhibits lower polymerization shrinkage stress compared to other low-viscosity (both conventional and bulk-fill) RBCs, as well as conventional high-viscosity RBCs [50]. However, in contrast to these findings, Park et al. [39] reported no disparity in the adaptation of SDR compared to other RBCs.

Regarding location and extent, our results aligned with other RBCs, showcasing comparable gap formation on the pulpal floor with SDR. Nonetheless, SDR was the only material where no internal gap was found on the lateral walls. Furness et al. similarly detected a substantial percentage of gap formation at the pulpal floor for SDR. Notably, their study also unveiled greater detachment along the lateral interface in the case of SDR compared to other investigated bulk-fill or incrementally placed RBCs [29].

The quality of the adhesive interface plays a pivotal role in internal adaptation. If adhesive bonding fails to counteract shrinkage stress, debonding may ensue [48]. Separation at the interface contributes to heightened shrinkage vectors, offering greater freedom for shrinkage movement [51]. To ensure comparability, a uniform one-step self-etch adhesive (G-Premio Bond, GC Europe) was employed in selective etching mode across all groups in this study. The occurrence of gap formation can be attributed to feeble bonding with dentin and/or robust bonding with enamel on the opposing cavity wall [30]. Among adhesive systems, one-step self-etch adhesives are recognized for providing comparatively weaker bond strength [52]. An additional rationale for our findings may lie in the diminished polymerization shrinkage stress exhibited by bulk-fill RBCs, which could favorably impact internal adaptation, particularly when coupled with underperforming adhesive systems like the one-step self-etch approach [39]. In contrast, the incremental technique, due to multiple photopolymerization stages and consequential contraction stress, along with amplified shrinkage vectors, may further compromise the already delicate dentin-RBC bonding. Shrinkage vectors predominantly manifest axial movement contingent upon bonding conditions. In cases of debonded RBCs, axial movement is directed upward toward the curing light, while bonded RBCs experience shrinkage from the free surface towards the cavity wall [53].

Three-dimensional high-resolution micro-computed tomography was also used for the volumetric assessment of closed porosity, leveraging the method's accuracy in quantitatively gauging and visualizing failures such as air bubbles [4]. Although air bubbles and voids can potentially infiltrate RBCs during manipulation, it is important to note that submicron pores are inherently present in RBCs as provided by the manufacturer [4]. Porosity stands as a parameter wielding influence over numerous properties of RBCs, thereby making the determination of closed porosity pertinent from both mechanical and chemical standpoints. Voids serve as defects, introducing a discontinuous phase to the RBC matrix, which has the potential to undermine mechanical properties [4]. From a chemical vantage, these pores harbor an oxygen-inhibited layer, potentially leading to heightened release of unreacted monomers [54]. Moreover, porosity can elevate the water absorption capacity of the RBC, thereby contributing to the previously detailed alterations in internal adaptation during the aging process [5]. The presence of voids has been observed to depend on factors such as RBC consistency, thickness, placement technique, and operator proficiency [55]. The outcomes of closed porosity measurement in this study unveiled a notably greater pore volume within the layered RBCs when contrasted with samples employing the bulk-fill approach. This observation aligns with certain findings in the literature [56,57], although it diverges from others [58]. Notably, while it has been documented that the utilization of flowable RBCs may lead to an augmented voids volume in restorations [59], our findings diverge from this notion. Specifically, we found no significant distinction between low and high viscosity bulk-fill groups, akin to the study conducted by Nilsen et al. [4].

Micro-Raman spectroscopy was employed to evaluate the degree of polymerization across the upper, middle, and lower surfaces. The polymerization of RBCs is profoundly influenced by various factors encompassing the resin monomer's chemical structure, filler attributes, photoinitiator type and concentration, layer thickness, opacity, and

polymerization conditions, among others [16]. To ensure comparability, the curing conditions in our study were standardized, affording a basis for comparing different materials in terms of internal adaptation and degree of conversion (DC). Among the investigated groups, G-aenial_Layered exhibited the highest mean DC% (87.2%), trailed by SDR_Bulk (81.2%), EverX_Layered (77.5%), and EverX_Bulk (75.8%). These DC values are notably high and were attained through prolonged exposure time. It is well-documented that a heightened degree of cure can be achieved by elevating energy density, primarily by extending the exposure time [22]. While EverX displayed the lowest DC values among the investigated groups, both EverX_Bulk and EverX_Layered demonstrated excellent depth of cure. Notably, no statistically significant differences in DC% were detected across various Raman detection regions (top, middle, and bottom) for these two EverX groups. Comparing the bulk and incremental application of EverX, the disparities in DC values were deemed insignificant between them. However, EverX_Bulk exhibited slightly lower DC% at the middle and bottom regions of the restoration. Our findings are in line with other research that highlights the enhanced light penetration of translucent SFRC, attributed to its glass fibers, compared to other RBCs, despite increased light scattering and absorption with greater layer thickness [60]. Garoushi et al. similarly reported that, akin to EverX Posterior, SDR demonstrated no substantial correlation between DC and layer thickness [60]. In our study, although SDR exhibited a notably high mean DC% at a 4 mm thickness, significant differences in DC were observed between the top, middle, and bottom regions. Furthermore, a significant discrepancy in DC between the top and bottom layers was evident for G-aenial when applied in 2 mm increments. Pearson correlation analysis highlighted a moderately strong association between DC and the application method. This suggests that layering in 2 mm increments tends to enhance the degree of polymerization compared to the bulk technique.

However, the role of the RBC's composition, the chemical and physical properties of the monomers, filler type and load, and initiator system, among others, is indisputable in the polymerization kinetics, as supported by the moderately large correlation between DC and material [41]. While high DC is preferred due to the advantageous resulting mechanical and chemical properties, DC was found to be in clinical contradiction with polymerization shrinkage [61]. Conversely, the influence of the curing mode (irradiance, exposure time) on DC, shrinkage strain, and consequently on IA has also been demonstrated [62]. By keeping the curing parameters constant, using the same settings (irradiance and exposure time) for each group, we were able to examine the effect of DC on IA. Although the highest IA was observed in relation to the highest DC in the case of G-aenial_Layered, SDR showed a much more favorable adaptation despite having a similarly high DC value. Considering the SFRC RBCs, while there was a slight, but not significant difference in DC between the bulk and layered groups, a remarkable discrepancy was detected in IA. Given the inconsistent results, the correlation analysis revealed an insignificant association between DC and IA. While a thinner composite layer is more advantageous in terms of conversion [16], it is supposed that the polymerization rate, and consequently the polymerization shrinkage of a 2 mm layer as opposed to a 4 mm thick increment, can lead to higher stress [63]. In bulk polymerization, shrinkage stress at the interfaces may be reduced due to the ability of unpolymerized RBC at the bottom to deform and release stress. However, in the incremental layering technique, more stress may arise from the absence of a deep reservoir of uncured RBC from which to relieve polymerization stresses of the upper composite segment [29]. In terms of DC, a bulk-fill RBC can also achieve a high level, attributed to the higher exothermic reaction reported in bulk-fills [19]. The heat released during polymerization can facilitate the mobility of reactive species, allowing for increased DC [64]. As demonstrated, low viscosity, greater layer thickness, and increased translucency (such as SDR_Bulk and EverX_Bulk) predispose to a more significant exothermic reaction and a higher degree of polymerization [19].

'Despite the careful sample preparation during our investigation, the destructive effects of tooth sectioning - such as thermal load, shear forces, fatigue, vibration, and structural changes among others - required for SEM and micro-Raman evaluation may affect the results, thus the findings of this in vitro restorative study must be carefully interpreted for an in vivo situation. Evaluation of tissues or their interfaces, such as dentin-RBC, can be accomplished only when these have been prepared with minimum to no artifacts. In order to minimize the effects influencing or modifying the results, the samples were stored in physiological saline solution in an incubator at 37 °C for one month to allow complete post-polymerization of the RBCs [65], to alleviate the stress due to water sorption [66], and to prevent dehydration of tooth, RBC and their adhesive interface [67]. To prevent thermal effect during specimen sectioning and polishing, which may cause structural degradation and influence the DC, constant irrigation was employed [68].

Although the samples being stored in saline for one month, another limitation of this study is the absence of thermo-mechanical loading. This can partially simulate the oral conditions that affect RBC restorations during function. Kim and Park demonstrated that internal adaptation deteriorated due to cyclic loading [1]. While a more pronounced deterioration is expected after thermo-mechanical loading, the differences between the examined groups were detectable even after one month of wet storage, as indicated by the results of the present study.

Furthermore, micro-CT imaging, while allowing a detailed display of interfacial adaptation detectable by X-ray, has a limitation of long measurement times that can lead to dehydration of specimens during scanning, resulting in deformation and false positives. This methodological sensitivity is also applicable to SEM examination, however, to reduce the undesirable changes, HMDS drying, as an alternative method was used to dry the samples [69]. Although vacuum sputter-coating may result in debonding as an artifact, SEM, as a visualization tool is a common and well-established method for investigating interfacial gap formation [32–34].

An additional challenge was posed by the delineation of the interface due to the very similar pixel intensity of the tooth, adhesive layer, and RBC on the micro-CT images. Despite these methodological limitations, micro-CT has proven to be a non-destructive and effective tool for quantitatively determining the volume of internal gaps and closed pores in RBC restorations [28,30,39].

5. Conclusions

Within the limitations of this *ex vivo* study, it can be concluded that bulk placement of RBCs exhibited lower interfacial gap volume and achieved satisfactory DC in deep cavities without significant correlation between these parameters. The interfacial gap and DC values were predominantly influenced by the RBC type and filling technique. The least interfacial detachment occurred in the teeth restored with the flowable bulk-fill RBC (SDR_Bulk). Incremental insertion of SFRC had no advantage over bulk placement in terms of IA and DC. Further data from various experiments including simulation of clinical conditions, different curing parameters, and applying distinct adhesive systems among others are necessary to investigate the potential clinical benefits of bulk vs. layered SFRCs.

Acknowledgments

This work was supported by the Hungarian Academy of Sciences Bolyai János Research Scholarship and BO/713/20/5); the ÚNKP-22–5 New National Excellence Program of the Ministry of Hungary for Innovation and Technology from the Source of the National Research, Development and Innovation Fund (ÚNKP-22-5-PTE-1733 and ÚNKP-22-5-SZTE-572); Thematic Excellence Program of the Ministry of Hungary (TKP2021-EGA-17); Economic Development and Innovation Operational Program of the Ministry of Hungary (GINOP-2.3.1-20-2020-00007) University of P é cs Medical School Research Fund (PTE-ÁOK-KA-2020/24).

Special thanks to Dr. Gábor Braunitzer for the English language correction.

Disclosure statement

The authors of the following manuscript (Relation between internal adaptation and degree of conversion of short-fiber reinforced resin composites applied in bulk or layered technique in deep MOD cavities) state, that the manuscript is not concurrently under consideration for publication in another journal, that all of the named authors were involved in the work leading to the publication of the paper, and that all the named authors have read the paper before it is submitted for publication.

References

[1] Kim HJ, Park SH. Measurement of the internal adaptation of resin composites using micro-CT and its correlation with polymerization shrinkage. Oper Dent 2014;39: E57–70.
[2] Néma V, Sáry T, Szántó FL, Szabó B, Braunitzer G, Lassila L, Garoushi S, Lempel E, Fráter M. Crack propensity of different direct restorative procedures in deep MOD cavities. Clin Oral Invest 2023;27:2003–11.
[3] Soares CJ, Faria-E-Silva AL, Rodrigues MP, Vilela ABF, Pfeifer CS, Tantbirojn D, Versluis A. Polymerization shrinkage stress of composite resins and resin cements - what do we need to know? Braz Oral Res 2017;31(suppl 1):e62.
[4] Nilsen BW, Mouhat M, Jokstad A. Quantification of porosity in composite resins delivered by injectable syringes using X-ray microtomography. Biomater Invest Dent 2020;7:86–95.
[5] Balthazard R, Jager S, Dahoun A, Gerdolle D, Engels-Deutsch M, Mortie E. High-resolution tomography study of the porosity of three restorative resin composites. Clin Oral Invest 2014;18:1613–8.
[6] Ratih DN, Palamara JE, Messer HH. Dentinal fluid flow and cuspal displacement in response to resin composite restorative procedures. Dent Mater 2007;23:1405–11.
[7] Ferracane JL, Hilton TJ. Polymerization stress–is it clinically meaningful? Dent Mater 2016;32:1–10.
[8] Braga RR, Boaro LC, Kuroe T, Azevedo CL, Singer JM. Influence of cavity dimensions and their derivatives (volume and 'C' factor) on shrinkage stress development and microleakage of composite restorations. Dent Mater 2006;22: 818–23.
[9] Forster A, Braunitzer G, Tóth M, Szabó BP, Fráter M. In vitro fracture resistance of adhesively restored molar teeth with different MOD cavity dimensions. J Prosthodont 2019;28:e325–31.
[10] Park J, Chang J, Ferracane J, Lee IB. How should composite be layered to reduce shrinkage stress: incremental or bulk filling? Dent Mater 2008;24:1501–5.
[11] Fronza BM, Rueggeberg FA, Braga RR, Mogilevych B, Soares LE, Martin AA, Ambrosano G, Giannini M. Monomer conversion, microhardness, internal marginal adaptation, and shrinkage stress of bulk-fill resin composites. Dent Mater 2015;31: 1542–51.
[12] Bucuta S, Ilie N. Light transmittance and micro-mechanical properties of bulk fill vs. conventional resin based composites. Clin Oral Invest 2014;18:1991–2000.
[13] Garoushi S, Säilynoja E, Vallittu PK, Lassila L. Physical properties and depth of cure of a new short fiber reinforced composite. Dent Mater 2013;29:835–41.
[14] Garoushi S, Gargoum A, Vallittu PK, Lassila L. Short fiber-reinforced composite restorations: A review of the current literature. J Invest Clin Dent 2018;9:e12330.
[15] Tezvergil A, Lassila LV, Vallittu PK. The effect of fiber orientation on the polymerization shrinkage strain of fiber-reinforced composites. Dent Mater 2006; 22:610–6.
[16] AlShaafi MM. Factors affecting polymerization of resin-based composites: a literature review. Saudi Dent J 2017;29:48–58.
[17] Moldovan M, Balazsi R, Soanca A, Roman A, Sarosi C, Prodan D, Vlassa M, Cojocaru I, Saceleanu V, Cristescu I. Evaluation of the degree of conversion, residual monomers and mechanical properties of some light-cured dental resin composites. Mater (Basel) 2019;12:2109.
[18] Lovász BV, Lempel E, Szalma J, Sétáló Jr G, Vecsernyés M, Berta G. Influence of TEGDMA monomer on MMP-2, MMP-8, and MMP-9 production and collagenase activity in pulp cells. Clin Oral Invest 2021;25:2269–79.
[19] Lempel E, Őri Zs, Kincses D, Lovász BV, Kunsági-Máté S, Szalma J. Degree of conversion and in vitro temperature rise of pulp chamber during polymerization of flowable and sculptable conventional, bulk-fill and short-fibre reinforced resin composites. Dent Mater 2021;37:983–97.
[20] Han SH, Park SH. Comparison of internal adaptation in Class II bulk-fill composite restorations using micro-CT. Oper Dent 2017;42:203–14.
[21] Alshali RZ, Silikas N, Satterthwaite JD. Degree of conversion of bulk-fill compared to conventional resin- composites at two time intervals. Dent Mater 2013;29: e213–7.
[22] Lempel E, Őri Zs, Szalma J, Lovász BV, Kiss A, Tóth Á, Kunsági-Máté S. Effect of exposure time and pre-heating on the conversion degree of conventional, bulk-fill, fiber reinforced and polyacid-modified resin composites. Dent Mater 2019;35: 217–28.
[23] Scotti N, Tempesta RM, Pasqualini D, Baldi A, Vergano EA, Baldissara P, Alovisi M, Comba A. 3D interfacial gap and fracture resistance of endodontically treated premolars restored with fiber-reinforced composites. J Adhes Dent 2020;22: 215–24.
[24] Padam S. Sample size for experimental studies. J Clin Prev Card 2012;1:88–93.
[25] Opdam NJM, van de Sande FH, Bronkhorst E, Cenci MS, Bottenberg P, Pallesen U, Gaengler P, Lindberg A, Huysmans MC, van Dijken JW. Longevity of posterior composite restorations: a systematic review and meta-analysis. J Dent Res 2014;93: 943–9.
[26] Abbas G, Fleming GJP, Harrington E, Shortall ACC, Burke FJT. Cuspal movement and microleakage in premolar teeth restored with a packable composite cured in bulk or in increments. J Dent 2003;31:437–44.
[27] Han SH, Sadr A, Tagami J, Park SH. Internal adaptation of resin composites at two configurations: Influence of polymerization shrinkage and stress. Dent Mater 2016; 32:1085–94.
[28] Han SH, Sadr A, Tagami J, Park SH. Non-destructive evaluation of an internal adaptation of resin composite restoration with swept-source optical coherence tomography and micro-CT. Dent Mater 2016;32:e1–7.
[29] Furness A, Tadros MY, Looney SW, Rueggeberg FA. Effect of bulk/incremental fill on internal gap formation of bulk-fill composites. J Dent 2014;42:439–49.
[30] Chiang YC, Rösch P, Dabanoglu A, Lin CP, Hickel R, Kunzelmann KH. Polymerization composite shrinkage evaluation with 3D deformation analysis from microCT images. Dent Mater 2010;26:223–31.
[31] Pashley DH, Pashley EL, Carvalho RM, Tay FR. The effects of dentin permeability on restorative dentistry. Dent Clin North Am 2002;46:211–45.
[32] Van Landuyt KL, Snauwaert J, De Munck J, Coutinho E, Poitevin A, Yoshida Y, Suzuki K, Lambrechts P, Van Meerbeek B. Origin of interfacial droplets with one-step adhesives. J Dent Res 2007;86:739–44.
[33] Tay FR, Pashley DH, Suh B, Carvalho R. and Miller M. Single-step, self-etch adhesives behave as permeable membranes after polymerization. Part I. Bond strength and morphologic evidence. Am J Dent 2004;17:271–8.
[34] Heintze SD, Monreal D, Peschke A. Marginal quality of class II composite restorations placed in bulk compared to an incremental technique: evaluation with SEM and stereomicroscope. J Adhes Dent 2015;17:147–54.
[35] Kaisarly D, El Gezawi M, Keßler A, Rösch P, Kunzelmann KH. Shrinkage vectors in flowable bulk-fill and conventional composites: bulk versus incremental application. Clin Oral Invest 2021;25:1127–39.
[36] Braga RR, Ballester RY, Ferracane JL. Factors involved in the development of polymerization shrinkage stress in resin-composites: A systematic review. Dent Mater 2005;21:962–70.
[37] Halvorson RH, Erickson RL, Davidson CL. Energy dependent polymerization of resin-based composite. Dent Mater 2002;18:463–9.
[38] Szczesio-Wlodarczyk A, Sokolowski J, Kleczewska J, Bociong K. Ageing of dental composites based on methacrylate resins - a critical review of the causes and method of assessment. Polym (Basel) 2020;12:882.
[39] Park KJ, Pfeffer M, Näke T, Schneider H, Ziebolz D, Haak R. Evaluation of low-viscosity bulk-fill composites regarding marginal and internal adaptation. Odontology 2021;109:139–48.
[40] Rosales-Leal JI, Castillo-Salmerón RD, Molino-Serrano MA, González-Moreira H, Cabrerizo-Vílchez MA. Effect of hygroscopic expansion of resin filling on interfacial gap and sealing: a confocal microscopy study. J Adhes Dent 2013;15:423–30.
[41] Gajewski VE, Pfeifer CS, Fróes-Salgado NR, Boaro LC, Braga RR. Monomers used in resin composites: degree of conversion, mechanical properties and water sorption/ solubility. Braz Dent J 2012;23:508–14.
[42] Ferracane JL. Hygroscopic and hydrolytic effects in dental polymer networks. Dent Mater 2006;22:211–22.
[43] Ito S, Hashimoto M, Wadgaonkar B, Svizero N, Carvalho RM, Yiu C, Rueggeberg FA, Foulger S, Saito T, Nishitani Y, Yoshiyama M, Tay FR, Pashley DH. Effects of resin hydrophilicity on water sorption and changes in modulus of elasticity. Biomaterials 2005;26:6449–59.
[44] Alshali RZ, Salim NA, Satterthwaite JD, Silikas N. Long-term sorption and solubility of bulk-fill and conventional resin-composites in water and artificial saliva. J Dent 2015;43:1511–8.
[45] Sideridou ID, Karabela MM, Bikiaris DN. Aging studies of light cured dimethacrylate-based dental resins and a resin composite in water or ethanol/ water. Dent Mater 2007;23:1142–9.
[46] Alshabib A, Algamaiah H, Silikas N, Watts DC. Material behavior of resin composites with and without fibers after extended water storage. Dent Mater J 2021;40:557–65.
[47] Oumer AN, Mamat O. A study of fiber orientation in short fiber-reinforced composites with simultaneous mold filling and phase change effects. Comp Part B: Eng 2012;43:1087–94.
[48] Kaisarly D, El Gezawi M, Xu X, Rösch P, Kunzelmann K-H. Shrinkage vectors of a flowable composite in artificial cavity models with different boundary conditions: ceramic and Teflon. J Mech Behav Biomed Mater 2018;77:414–21.
[49] Ilie N, Kessler A, Durner J. Influence of various irradiation processes on the mechanical properties and polymerisation kinetics of bulk-fill resin based composites. J Dent 2013;41:695–702.
[50] Rizzante FAP, Mondelli RFL, Furuse AY, Borges AFS, Mendonça G, Ishikiriama SK. Shrinkage stress and elastic modulus assessment of bulk-fill composites. J Appl Oral Sci 2019;27:e20180132.
[51] Kaisarly D, El Gezawi M, Lai G, Jin J, Rösch P, Kunzelmann K-H. Effects of occlusal cavity configuration on 3D shrinkage vectors in a flowable composite. Clin Oral Invest 2018;22:2047–56.
[52] El Gedaily M, Attin T, Wiedemeier DB, Tauböck TT. Impact of different etching strategies on margin integrity of conservative composite restorations in demineralized enamel. Mater (Basel) 2020;13:4500.

[53] Van Ende A, Van de Casteele E, Depypere M, De Munck J, Li X, Maes F, Wevers M, Van Meerbeek B. 3D volumetric displacement and strain analysis of composite polymerization. Dent Mater 2015;31:453–61.
[54] Gauthier MA, Stangel I, Ellis TH, Zhy XX. Oxygen inhibition in dental resins. J Dent Res 2005;84:725–9.
[55] Samet N, Kwon KR, Good P, Weber HP. Voids and interlayer gaps in class 1 posterior composite restorations: a comparison between a microlayer and a 2-layer technique. Quintessence Int 2006;37:803–9.
[56] Soares CJ, Rosatto C, Carvalho VF, Bicalho AA, Henriques J, Faria-E-Silva AL. Radiopacity and porosity of bulk-fill and conventional composite posterior restorations-digital X-ray analysis. Oper Dent 2017;42:616–25.
[57] Dunavári E, Berta G, Kiss T, Szalma J, Fráter M, Böddi K, Lempel E. Effect of pre-heating on the monomer elution and porosity of conventional and bulk-fill resin-based dental composites. Int J Mol Sci 2022;23:16188.
[58] Soto-Montero J, Giannini M, Sebold M, de Castro EF, Abreu JLB, Hirata R, Dias CTS, Price RBT. Comparison of the operative time and presence of voids of incremental and bulk-filling techniques on Class II composite restorations. Quintessence Int 2022;53:200–8.
[59] Pardo Díaz CA, Shimokawa C, Sampaio CS, Freitas AZ, Turbino ML. Characterization and comparative analysis of voids in Class II composite resin restorations by optical coherence tomography. Oper Dent 2020;45:71–9.
[60] Garoushi S, Vallittu P, Shinya A, Lassila L. Influence of increment thickness on light transmission, degree of conversion and micro hardness of bulk fill composites. Odontology 2016;104:291–7.
[61] Amirouche-Korichi A, Mouzali M, Watts DC. Effects of monomer ratios and highly radiopaque fillers on degree of conversion and shrinkage-strain of dental resin composites. Dent Mater 2009;25:1411–4.
[62] Silikas N, Eliades G, Watts DC. Light intensity effects on resin-composite degree of conversion and shrinkage strain. Dent Mater 2000;16:292–6.
[63] Xu T, Li X, Wang H, Zheng G, Yu G, Wang H, Zhu S. Polymerization shrinkage kinetics and degree of conversion of resin composites. J Oral Sci 2020;62:275–80.
[64] Par M, Gamulin O, Marovic D, Klaric E, Tarle Z. Effect of temperature on post-cure polymerization of bulk-fill composites. J Dent 2014;42:1255–60.
[65] Braga S, Schettini A, Carvalho E, Shimokawa C, Price RB, Soares CJ. Effect of the sample preparation and light-curing unit on the microhardness and degree of conversion of bulk-fill resin-based composite restorations. Oper Dent 2022;47:163–72.
[66] Bociong K, Szczesio A, Sokolowski K, Domarecka M, Sokolowski J, Krasowski M, Lukomska-Szymanska M. The influence of water sorption of dental light-cured composites on shrinkage stress. Materials 2017;10:1142.
[67] Zhang D, Mao S, Lu C, Romberg E, Arola D. Dehydration and the dynamic dimensional changes within dentin and enamel. Dent Mater 2009;25:937–45.
[68] Lohbauer U, Pelka M, Belli R, Schmitt J, Mocker E, Jandt KD, Müller FA. Degree of conversion of luting resins around ceramic inlays in natural deep cavities: a micro-Raman spectroscopy analysis. Oper Dent 2010;35(5):579–86.
[69] Perdigao J, Lambrechts P, Van Meerbeek B, Vanherle G, Lopes AL. Field emission SEM comparison of four postfixation drying techniques for human dentin. J Biomed Mater Res 1995;29:1111–20.